Synthesis and Photophysical Properties of Soluble Low-Bandgap Thienothiophene Polymers with Various Alkyl Side-Chain Lengths

WOO JIN BAE,[1,2] CHRISTOPHER SCILLA,[1] VOLODIMYR V. DUZHKO,[1,3] WON HO JO,[2] E. BRYAN COUGHLIN[1]

[1]Department of Polymer Science and Engineering, University of Massachusetts Amherst, Conte Center for Polymer Research, 120 Governors Drive, Amherst, Massachusetts 01003

[2]Department of Materials Science and Engineering, Seoul National University, Seoul 151-742, Republic of Korea

[3]Energy Frontier Research Center PHaSE, University of Massachusetts, Amherst, Massachusetts 01003

Received 6 April 2011; accepted 30 April 2011
DOI: 10.1002/pola.24761
Published online 27 May 2011 in Wiley Online Library (wileyonlinelibrary.com).

ABSTRACT: We report the facile synthesis and characterization of a class of thienothiophene polymers with various lengths of alkyl side chains. A series of 2-alkylthieno[3,4-*b*]thiophene monomers (Ttx) have been synthesized in a two-step protocol in an overall yield of 28–37%. Poly(2-alkylthieno[3,4-*b*]thiophenes) (PTtx, alkyl: pentyl, hexyl, heptyl, octyl, and tridecyl) were synthesized by oxidative polymerization with $FeCl_3$ or via Grignard metathesis (GRIM) polymerization methods. The polymers are readily soluble in common organic solvents. The polymers synthesized by GRIM polymerization method (PTtx-G) have narrower molecular weight distribution ($Đ$) with lower molecular weight (M_n) than those synthesized by oxidative polymerization (PTtx-O). The band structures of the polymers with various lengths of alkyl side chains were investigated by UV–vis spectroscopy, cyclic voltammetry, and ultraviolet photoelectron spectroscopy. These low-bandgap polymers are good candidates for organic transistors, organic light-emitting diodes, and organic photovoltaic cells. © 2011 Wiley Periodicals, Inc. J Polym Sci Part A: Polym Chem 49: 3260–3271, 2011

KEYWORDS: conjugated polymers; electrochemistry; Grignard metathesis polymerization; low bandgap; oxidative polymerization; thienothiophene; ultraviolet photoelectron spectroscopy; UV-Vis spectroscopy

INTRODUCTION In the past 2 decades, considerable interest in the synthesis and properties of tailored conjugated polymers has emerged because of their potential use in optoelectronic devices, such as light-emitting diodes,[1] lasers,[2] field-effect transistors,[3] and photovoltaic cells.[4,5] The band structure of semiconducting polymers dictates their electrochemical, optical, and charge-carrier transport properties. The band structure can be tuned by altering either, or both, the electronic structure and sterics of the backbone.[6] Of particular interest is the preparation of stable, low-bandgap semiconducting polymers. These materials have attracted much attention because of their high visible transmissivity in the conductive form and their ease with which they can be either p- or n-doped.[7] The emergence of organic solar cells has given a greater impetus to conducting research to develop new conjugated polymers. Low-bandgap semiconducting polymer/fullerene bulk heterojunction solar cells have received growing attention because of their potential to extend the absorption of the solar spectrum to the near infrared region.[8,9] Theoretically, the resultant increase in short-circuit current makes it possible to achieve 10% power conversion efficiency (PCE).[10] Thus, low bandgap ($E_g < 1.8$ eV) polymers are of crucial importance for realizing the commercialization of low-cost polymer photovoltaics.[11] The bandgap of conjugated polymers is known to be determined by several factors, that is, aromaticity and bond-length alternation, chemical rigidification, stereoregularity-induced interchain coupling, inductive effects, and intramolecular charge transfer between alternating donors and acceptors. By properly considering all of these factors, the design of conjugated polymers can be tailored to reduce the bandgap.[12]

The synthesis and characterization of low-bandgap polymers date back to the mid-1980s, and there are several known strategies for synthesizing these materials.[13] The first low-bandgap polymer reported was poly(isothianaphthene) (ITN) ($E_g = 1.0$–1.2 eV), making the bandgap ~1 eV lower than that of polythiophene.[14] Like ITN, with its thiophene-fused benzene ring,[15–19] thienothiophene (Tt) has a thiophene ring fused with another thiophene ring at the 3,3′ positions. Polythieno[3,4-*b*]thiophene (PTt) is capable of stabilizing the quinoid form of the main chain, resulting in a very low bandgap of 0.84 eV accompanied by good electrochemical stability.[20] Recently, the ester-substituted thieno[3,4-*b*]thiophene, which renders it both soluble and oxidatively stable, was

Additional Supporting Information may be found in the online version of this article. Correspondence to: E. B. Coughlin (E-mail: coughlin@mail.pse.umass.edu)

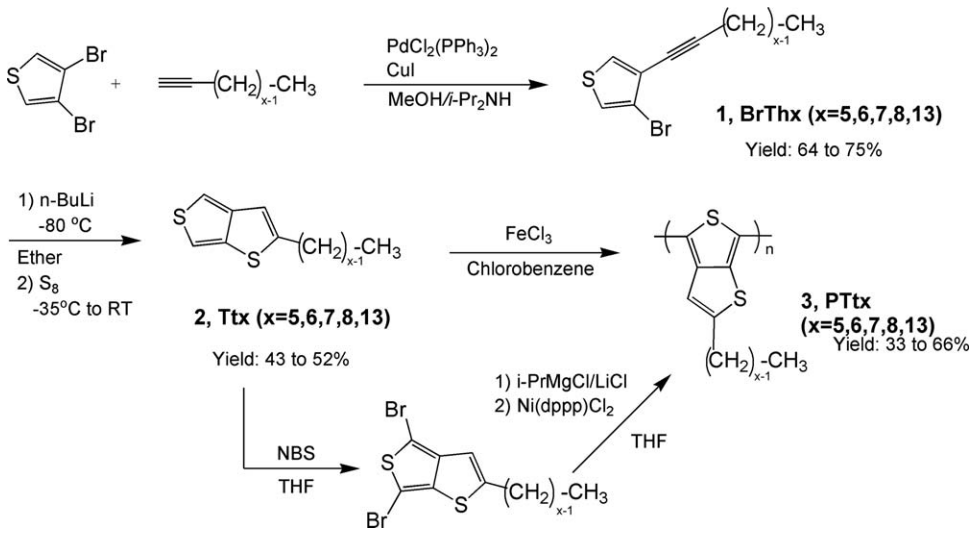

FIGURE 1 Synthetic route for monomer (Ttx) and polymer (PTtx).

copolymerized with dialkoxyl benzodithiophene resulting in a moderate bandgap material (~1.62 eV), which exhibited PCE of 5.6% when [6,6]-phenyl-C61-buyric acid methyl ester was used as an acceptor.[21] When a ketone-substituted thieno[3,4-*b*]thiophene was used instead of the ester-substituted Tt, the PCE increased to 6.3% as the highest occupied molecular orbital (HOMO) level of the copolymer was reduced by the removal of the oxygen atom on the ester group in the thieno[3,4-*b*]thiophene units.[22] The synthesis of organic soluble Tt in both cases is complicated by the fact that four synthetic steps are required. For the higher open-circuit voltage (V_{oc}) and lower HOMO level, alkyl-substituted Tt would be much more favorable because it is commonly known that alkoxy groups have much stronger electron-donating effect than alkyl groups. The synthesis of 2-decylthieno[3,4-*b*]thiophene has been reported in the literature,[23,24] and the bandgap of a film of the oxidized polymer was found to be about 1.2 eV. Unfortunately, the synthesis of this monomer is complicated in that it requires six steps.

A simple synthetic strategy was developed for nonsubstituted thieno[3,4-*b*]thiophene.[13,25] The synthesis of thieno [3,4-*b*] thiophene from 3,4-dibromothiophene was carried out in a manner analogues to Brandsma's procedure.[26] The first step involved palladium-catalyzed coupling of 3,4-dibromothiophene with trimethylsilylacetylene to produce 3-bromo-4-(trimethylsilyl)ethynylthiophene. Heterocyclic ring closure of 3-bromo-4-(trimethylsilyl)ethynylthiophene resulted in nonsubstituted thieno[3,4-*b*]thiophene. In spite of the simpler synthesis and higher overall yield, the resulting monomer is insoluble in common organic solvents and can be only polymerized by electrochemical method. Very recently, thieno[3,4-*b*]thiophene derivatives were synthesized by a two-step method utilizing catalytic amounts of CuO nanoparticles in the highest overall yield (14–20%) reported in the literature to date, and the optoelectronic properties of the resulting polymers synthesized by electrochemical polymerization were investigated.[27,28]

Herein, we report the facile synthesis and characterization of 2-alkylthieno[3,4-*b*]thiophene monomers (Ttx) with various lengths of side chains (alkyl = pentyl, hexyl, heptyl, octyl, and tridecyl). The monomer syntheses involve two steps, and the overall yields are in the range of 28–37%, which are, to the best of our knowledge, the highest reported to date. Alkyl-substituted poly(thieno[3,4-*b*]thiophenes) (PTtx) were synthesized by oxidative polymerization with $FeCl_3$ or by Grignard metathesis (GRIM) polymerization methods. The resulting polymers are readily soluble in organic solvents. The bandgap and HOMO/LUMO levels of the resulting polymers with various alkyl chains were determined by combining UV–vis absorption, cyclic voltammetry (CV), and ultraviolet photoelectron spectroscopy (UPS) characterization techniques.

RESULTS AND DISCUSSION

Monomer and Polymer Synthesis and Characterization

Low-bandgap polymers (PTtx) were synthesized to explore the side-chain effects on bandgap, optical, electrical, and electrochemical properties. The streamlined synthetic route developed for preparation of the monomers and polymers is shown in Figure 1.

The first step involves the selective Sonogashira coupling of terminal alkynes with 3,3′-dibromothiophene to afford BrThx (**1**) as the major product (yield: 64–75%) in accordance with the procedure reported by Brandsma.[26] The second step for Ttx preparation involves two reactions, low-temperature lithium-halogen exchange using *n*-butyllithium (*n*-BuLi) followed by the addition of elemental sulfur. These reactions can be performed sequentially in a single flask by raising the temperatures from −80 °C after the first step to −35 °C to effect the ring-closing reaction. This two-step sequence occurred efficiently giving the monomers Ttx with yields in the range of 33–66%. The full characterization data for all Ttx monomers are provided in the Supporting Information.

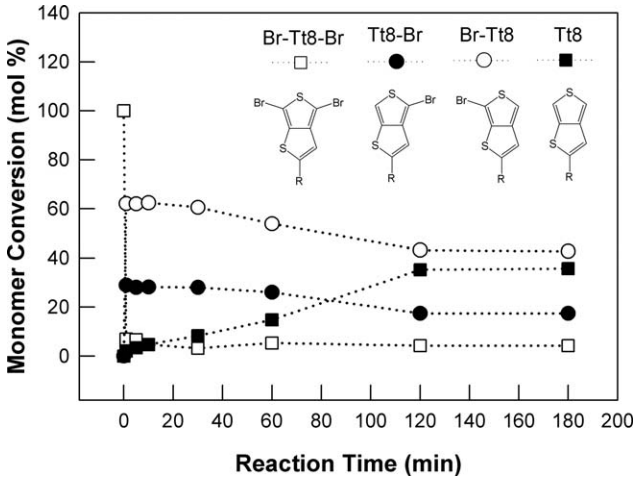

FIGURE 2 Conversion of monomer concentration versus time plots for magnesium halogen exchange of 4,6-dibromo-2-octylthieno[3,4-*b*]thiophene.

A monomer solution of dibromo Tt8 in tetrahydrofuran (THF) was allowed to react with the Grignard reagent, *i*Pr-MgCl, then quenched with water, and the products were analyzed by ^{1}H NMR. A time versus conversion plot is shown in Figure 2. After reaction for 1 min, almost all of the dibromomonomer (Br-Tt8-Br) was consumed, and only 7% remained. Considering that magnesium halogen exchange reaction of 9,9-dioctyl-2,7-dibromofluorene or 2,5-dibromo-3-hexylthiophene with various Grignard reagents usually takes several hours to reach 90% conversion of monosubstituted compound and disubstituted compound is difficult to be detected after several hours of reaction,[29–31] the reactivity of Br-Ttx-Br is much faster than other dibromomonomers in that the main components of the reaction mixture were 6-bromo-2-octylthieno[3,4-*b*]thiophene (Tt8-Br) and 6-bromo-2-octylthieno[3,4-*b*]thiophene (Br-Tt8) regioisomers (91%) after 1 min of reaction and 2% of disubstituted monomer (MgCl-Tt8-MgCl) was also detected at very early stages of reaction. The concentration of disubstituted monomer keeps increasing up to 35% for 2 h and does not change after further reaction as shown in Figure 2. Contrary to other disubstituted monomers, the concentration of either monosubstituted monomer (Br-Tt8 or Tt8-Br) keeps decreasing and reaches 60% after 2 h.

Polythienothiophene polymers (PTtx) were prepared by oxidative polymerization using $FeCl_3$ or by GRIM polymerization. After polymerization, precipitation in MeOH/water, and filtering, PTtx was further purified by Soxhlet extraction using MeOH, acetone, hexane, and $CHCl_3$. A small portion of hydrazine hydrate was added to the $CHCl_3$ solution and stirred overnight to reduce any oxidized species, and then the product was precipitated in MeOH/water and collected by filtration. Sample characterization was performed after the purification and fractionation steps. PTtx polymers prepared by either method are readily soluble in common organic solvents, such as $CHCl_3$, toluene, THF, 1,2-dichlorobenzene, and chlorobenzene, at room temperature. ^{1}H and ^{13}C NMR spectra, mass spectra data, and FTIR spectra of the resulting monomers and polymers were obtained for structural confirmation (Supporting Information). The number-average molecular weight (M_n), dispersity ($Đ$), and decomposition temperature (T_d) of PTtx samples are listed in Table 1.

The molecular weight of the polymers synthesized by oxidative polymerization (PTtx-O) is relatively high compared to that of the polymers synthesized via GRIM polymerization method (PTtx-G); however, the dispersity is much broader than that obtained by GRIM polymerization method, which is attributed to the characteristic of step-growth polymerization. Although PTtx-G has much narrower dispersity because of the quasi-living chain-growth characteristic of GRIM polymerization, the molecular weight is relatively low compared to PTtx-O. This lower molecular weight of PTtx-G is mainly due to the low yield of regioselective GRIM before catalyst addition. As α and β positions on thienothiophene ring are nearly chemically equivalent (Supporting Information Fig. 2*S*), a chance to react with isopropylmagnesium chloride (*i*Pr-MgCl) on both side is almost the same, which results in the magnesium-bromine exchange reaction on both bromine of 4,6-dibromo-2-alkyl-thieno[3,4-*b*]thiophene (Br-Ttx-Br), and consequently preventing the further chain growth by termination during polymerization. The chemical equivalence on both sides before and after bromination can also rule out the possibility of regioregularity of PTtx (Supporting Information Fig. 2*S*) by either method (GRIM or oxidative polymerization), which was already noted by the broad proton resonance around δ 7.0 ppm from ^{1}H NMR spectrum.

UV–Vis Characterization of PTtx

The optical absorption spectra of PTtx-O and PTtx-G in chloroform solution or as films on a glass substrate are shown in Figures 3 and 4, respectively. The spin-coated films of the PTtx look very uniform and do not have pinholes defect, regardless of the molecular weight (from 1.2 to 81 kg/mol). Interestingly, as the alkyl side-chain length of PTtx-O increases from 5 to 7, λ_{max} decreases in solution and in the solid state, and the optical bandgap calculated from the band edge increases as shown in Figure 3 and Table 2. However, as the alkyl side-chain length becomes longer than 7, the inverse effect was observed. Generally, poly(3-alkylthiophene) (P3ATs) with longer alkyl side chains have longer

TABLE 1 Molecular Characteristics of PTtx

	Oxidative Polym. (PTtx-O)			GRIM Polym. (PTtx-G)		
Sample	M_n (kg/mol)	$Đ$	T_d[a]	M_n (kg/mol)	$Đ$	T_d[a]
PTt5	30	18.2	263	4.3	1.1	290
PTt6	44	16.0	282	4.1	1.3	312
PTt7	15	20.2	247	5.7	1.2	326
PTt8	70	8.3	276	5.2	1.3	324
PTt13	81	27.9	285	–	–	–

[a] The 5 wt % weight-loss temperatures under inert atmosphere.

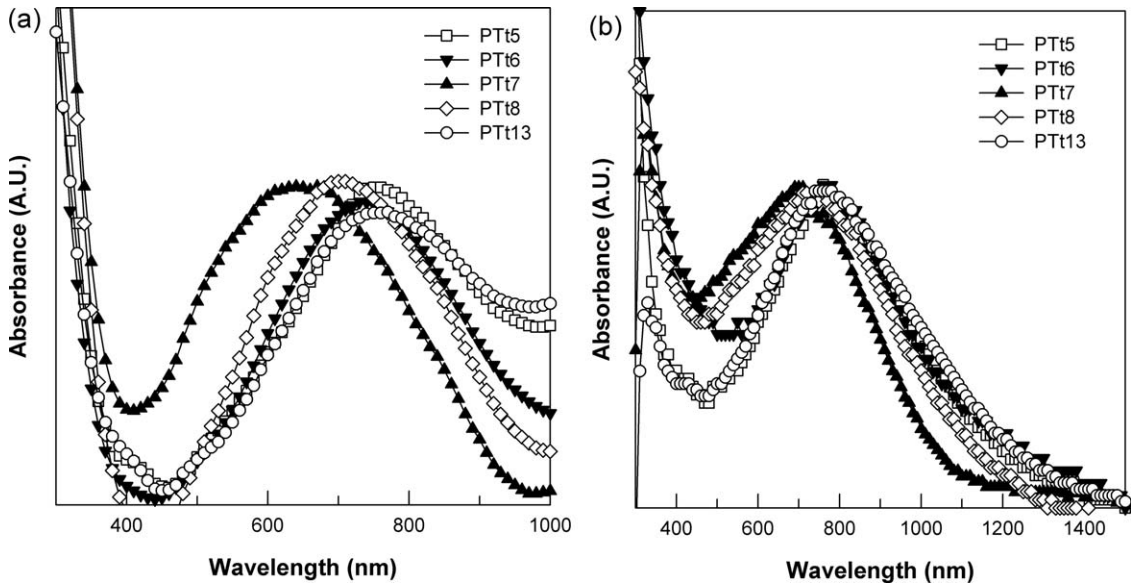

FIGURE 3 UV–vis–NIR absorption spectra of PTtx ($x = 5, 6, 7, 8, 13$) synthesized by oxidative polymerization (PTtx-O) in (a) $CHCl_3$ solution and as (b) films on a glass substrate.

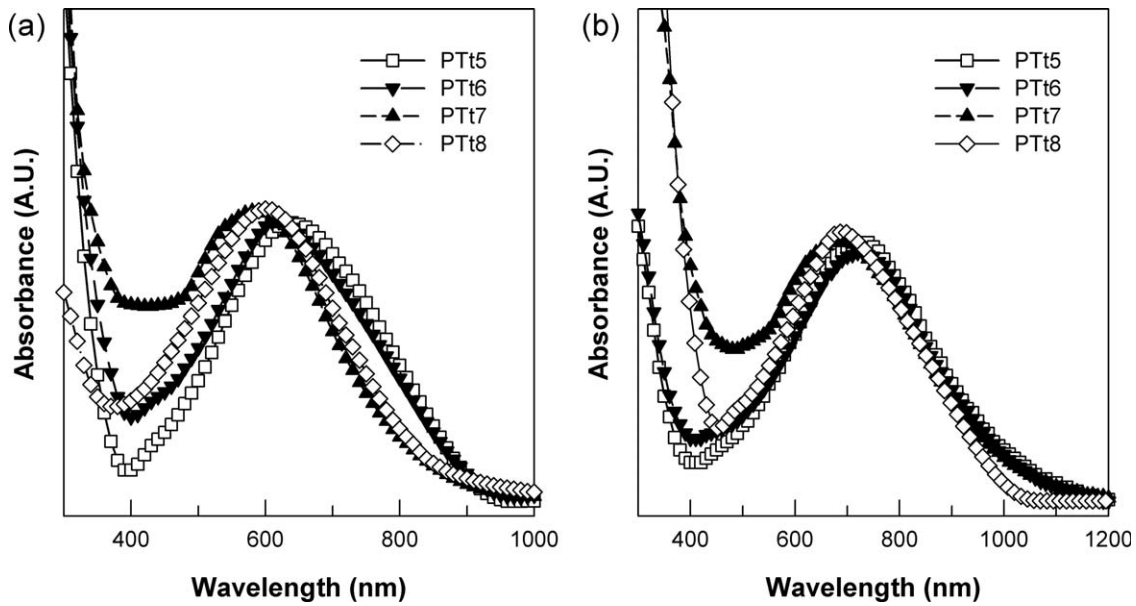

FIGURE 4 UV–vis–NIR absorption spectra of PTtx ($x = 5, 6, 7, 8$) synthesized by GRIM polymerization (PTtx-G) in (a) $CHCl_3$ solution and as (b) films on a glass substrate.

TABLE 2 Optical Properties of PTtx

	(PTtx-O) Absorption			(PTtx-G) Absorption		
Sample	λ_{max} ($CHCl_3$) (nm)	λ_{max} (Film) (nm)	E_g(opt) (Film) (eV)	λ_{max} ($CHCl_3$) (nm)	λ_{max} (Film) (nm)	E_g(opt) (Film) (eV)
PTt5	755	760	1.0	637	758	1.1
PTt6	735	748	1.0	616	749	1.2
PTt7	673	720	1.2	588	701	1.2
PTt8	703	755	1.2	603	693	1.3
PTt13	764	762	1.1	–	–	–

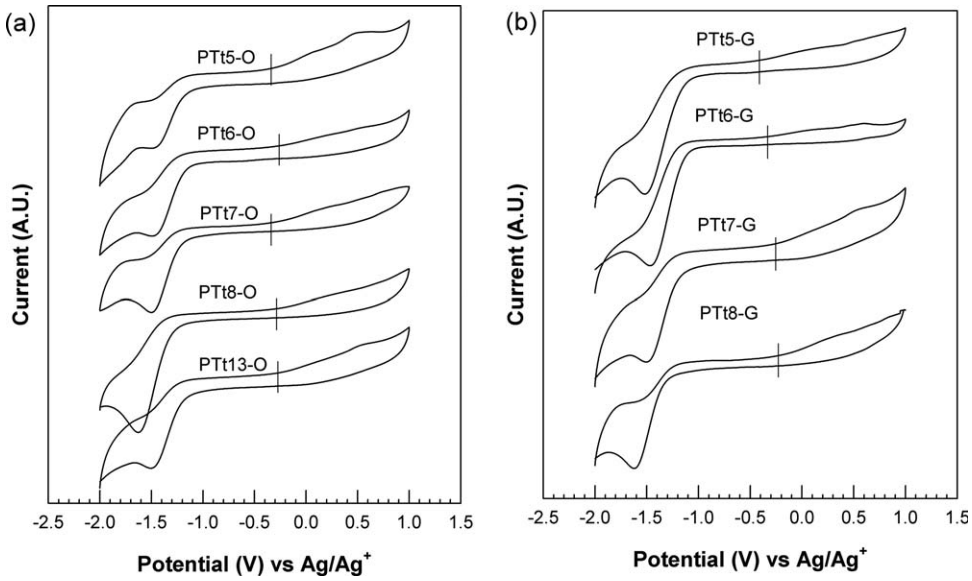

FIGURE 5 Cyclic voltammograms of (a) PTtx-O and (b) PTtx-G in 0.1 M Bu_4NBF_4 in dichloromethane (DCM). Ferrocene HOMO level was used as a reference. Ferrocene oxidation potential experimentally measured in the same electrolyte solution is 0.1 V (E_{vac} of ferrocene = 4.8 eV).

π-conjugation lengths leading to improved side-chain ordering.[32,33] Thus, our result is in the opposite direction of the P3ATs reported in the literature, but other reports on 2-alkoxy-5-methoxy poly(1,4-phenylenevinylene) derivatives with different lengths of the alkoxy side chain show similar trend like our PTtx series.[34] This effect is also observed in the UV–vis spectra of PTtx-G, as shown in Figure 4 and Table 2. Although λ_{max} and band edge of PTtx-G in solution or in the solid state are hypsochromically shifted compared to those of PTtx-O because of the difference in molecular weight between PTtx-O and PTtx-G, the trend of decrease in λ_{max} and increase in optical bandgap according to increase in alkyl side-chain length is analogous. One possible explanation for the decrease in λ_{max} and increase in optical bandgap as the alkyl side-chain length increases is the steric hindrance from the side chains. As the side-chain length increases from 5 to 7, the effect of steric hindrance makes the adjacent thiophene rings twist with respect to each other leading to shorter π-conjugation lengths and lower degree of aggregate formation. However, as the side-chain length becomes longer, the solvation of the side chains becomes predominant. Thus, the PTtx chains are solvated more favorably by solvent molecules as the length of the alkyl side chains increases. This can make the PTtx chains with longer alkyl side chains have a more expanded structure in solution.

When the maximum absorption of the polymers in solution is compared with that in solid state [Fig. 3(a) vs. (b) and Fig. 4(a) vs. (b)], the maximum absorption wavelengths (λ_{max}) of PTt5, PTt6, PTt7, and PTt8 are red shifted in the solid state compared to the solution (Table 2), indicating that polymer chains are associated in the solid state. When the λ_{max} difference between solution and solid state is compared between PTtx-O and PTtx-G, the difference is much smaller in PTtx-O (<50 nm) than in PTtx-G (~100 nm), which means the electronic structure of PTtx-O in solution is much closer to that in solid state. This can be explained by the aggregation of PTtx-O in solution state. As the molecular weight of PTtx-O increases, there is the possibility of aggregation by physical entanglement between adjacent polymer chains in solution or a self-collapsed coil structure. This assumption is supported by dynamic light scattering (DLS) characterization as shown in the Supporting Information (Supporting Information Fig. 10S). As PTtx-O exists as 10- to 100-nm nanosized aggregates in solution, the electronic structure in the solid state is not significantly enhanced compared to PTtx-G. On the other hand, PTtx-G in $CHCl_3$ solution does not show any scattering peak.

Electrochemical Property of PTtx

Electrochemical CV was performed to determine the HOMO/LUMO level and corresponding bandgaps of PTtx using a reported method.[35]

To determine the onset of the oxidation potential clearly, the cyclic voltammogram was initiated at a potential of −1.0 V and scanned in the positive direction. In both polymers (PTtx-O or PTtx-G), the oxidation peaks are very weak compared to the reduction peaks, which make it difficult to determine the onset point of oxidation (Fig. 5). A weak oxidation peak is usually observed in thienothiophene polymers.[27,28] The onset point was confirmed after expansion of the graph, and all the data are summarized in Table 3. Upon potential reversal at 1.0 V and further scanning in the cathodic direction, reductive process occurs with an onset of −1.1 to −1.3 V and a peak at −1.4 to −1.6 V. This has been commonly attributed to the injection of electrons or n-doping of the neutral conjugated polymer. The oxidation and reduction of PTtx (PTtx-O or PTtx-G) are very stable, and there is no loss of electroactivity observed upon cycling the potential 30 times.

Although the bandgap measured by electrochemical method is smaller than that by optical method, the trend of bandgap

TABLE 3 HOMO/LUMO Level and Bandgap of PTtx Measured by Electrochemical Method

	PTtx-O			PTtx-G		
Sample	HOMO[a] (eV)	LUMO[a] (eV)	E_g(ec)[b] (eV)	HOMO[a] (eV)	LUMO[a] (eV)	E_g(ec)[b] (eV)
PTt5	−4.35	−3.45	0.9	−4.30	−3.50	0.8
PTt6	−4.45	−3.45	1.0	−4.40	−3.50	0.9
PTt7	−4.40	−3.40	1.0	−4.40	−3.40	1.0
PTt8	−4.50	−3.30	1.2	−4.45	−3.25	1.2
PTt13	−4.50	−3.50	1.0	–	–	

[a] The energy levels were calculated using the following equation: HOMO $= -[E_{ox} - E_{1/2}(\text{ferrocene}) + 4.8]$ V and LUMO $= -[E_{rd} - E_{1/2}(\text{ferrocene}) + 4.8]$ V, where E_{ox} and E_{rd} are the onset oxidation potential and reduction potential of polymer, respectively, and $E_{1/2}$(ferrocene) is the onset oxidation potential of ferrocene versus Ag/Ag^+.

[b] Calculated by HOMO/LUMO difference measured by electrochemical method.

variation according to alkyl side-chain lengths is the same. Overall, the bandgap increases as the alkyl side-chain length increases at shorter chain lengths (R = 5–8), but when solvation is dominant at higher alkyl chain lengths (R = 13), the bandgap decreases because of the extended chain conformation. The HOMO level of PTtx according to the alkyl side-chain lengths does not seem to have a significant difference, considering the error is ±0.05 eV. Otherwise, the direct comparison of the HOMO level between PTt5 and PTt8 or PTt13 obtained by either polymerization method gives significant difference in HOMO level (0.15 eV difference). The slight decrease in HOMO level according to the increase in alkyl side-chain lengths is observed, which will be addressed in more detail by UPS measurements in the next section. HOMO/LUMO levels can give some criteria on how to design the energy level of the inner active layer materials for high-efficiency solar cell devices. Here, we note that both HOMO and LUMO levels of PTtx are shifted toward higher energy when compared with the ideal HOMO/LUMO level for a donor polymer (−3.9 to −4.0 eV and −5.3 to −5.8 eV for LUMO and HOMO level, respectively) in devices using PCBM as an acceptor.[10]

Ultraviolet Photoelectron Spectroscopy Characterization of PTtx

For an accurate measurement of HOMO levels, UPS studies were performed on PTtx-O. Frequently, CV does not give discrete values of HOMO and LUMO levels, because only reduction or oxidation is observed or only one process is found to be reversible in the case of many conjugated polymers.[36,37] UPS can provide information on the density of occupied electronic states and, therefore, allows for determining the energy of HOMO levels. In combination with the UV–vis–NIR absorption measurements, the energy of LUMO levels can be estimated as well. As the substrate can affect the electronic structure of the ultra-thin polymer film, PTt13 was spin coated on silver or heavily doped silicon wafer. In the case of poly(3-hexylthiophene) (P3HT), the choice of substrate can affect the morphology of the film, which results in a change of the electronic structure.[38] The HOMO levels of PTt13 on Si and Ag were determined to be −4.37 and −4.10 eV, respectively. The ionization potential of Si substrate and the Fermi level of Ag substrate without polymer film were −5.2 and −4.45 eV, respectively, which agrees with the reported literature values.[35,39] As the energy level of PTt13 on silicon wafer gives closer value to the energy level measured by electrochemical method (−4.5 eV), silicon substrates were further chosen for the UPS measurements, and PTtx-O with different alkyl side-chain lengths was spin coated on heavily doped silicon substrates with the thickness less than 10 nm. The UPS spectra of PTtx-O are shown in Figure 6.

The HOMO level was calculated using $-(21.2\text{ eV} - (E_1 - E_2))$, where E_1 is the secondary electron cutoff energy and E_2 is the high kinetic energy onset. The HOMO levels of PTtx-O are −4.05, −3.90, −4.08, −4.23, and −4.37 eV for PTt5, PTt6, PTt7, PTt8, and PTt13, respectively. The HOMO level variation of PTtx-O according to alkyl side-chain lengths roughly agrees with the results from electrochemical measurement. As it has been common practice to estimate LUMO level by subtraction of the optical bandgap from HOMO level determined either electrochemically or via optical absorption spectra,[40–42] here we show the energy band diagram derived from UPS and UV–vis measurement [Fig. 7(a)] and band diagram derived from electrochemical measurement [Fig. 7(b)] for comparison. Typically, the HOMO energy measured by UPS technique is slightly different compared to that measured by electrochemical methods.[43] The origin of this difference has been previously discussed and can be calculated from the equation, $E_{HOMO} = -(1.4 \pm 0.1)qV_{CV} - (4.6 \pm 0.08)$ eV for a wide range of organic electronic materials, where V_{CV} is oxidation potential measured by electrochemical method and E_{HOMO} is directly measured from the UPS spectrum.[43] Similarly, an empirical relation between the LUMO energies determined from either the electrochemical method or optical techniques was proposed.[44] In both types of measurement (UPS or CV), the alkyl side-chain lengths not only affect the bandgap but also affect the HOMO level of the PTtx.

Thermal Properties of PTtx

Thermal stability of PTtx was investigated with thermogravimetric analysis (TGA), as thermal stability is an important property of conjugated polymers to be used for electronic and optoelectronic applications. The decomposition

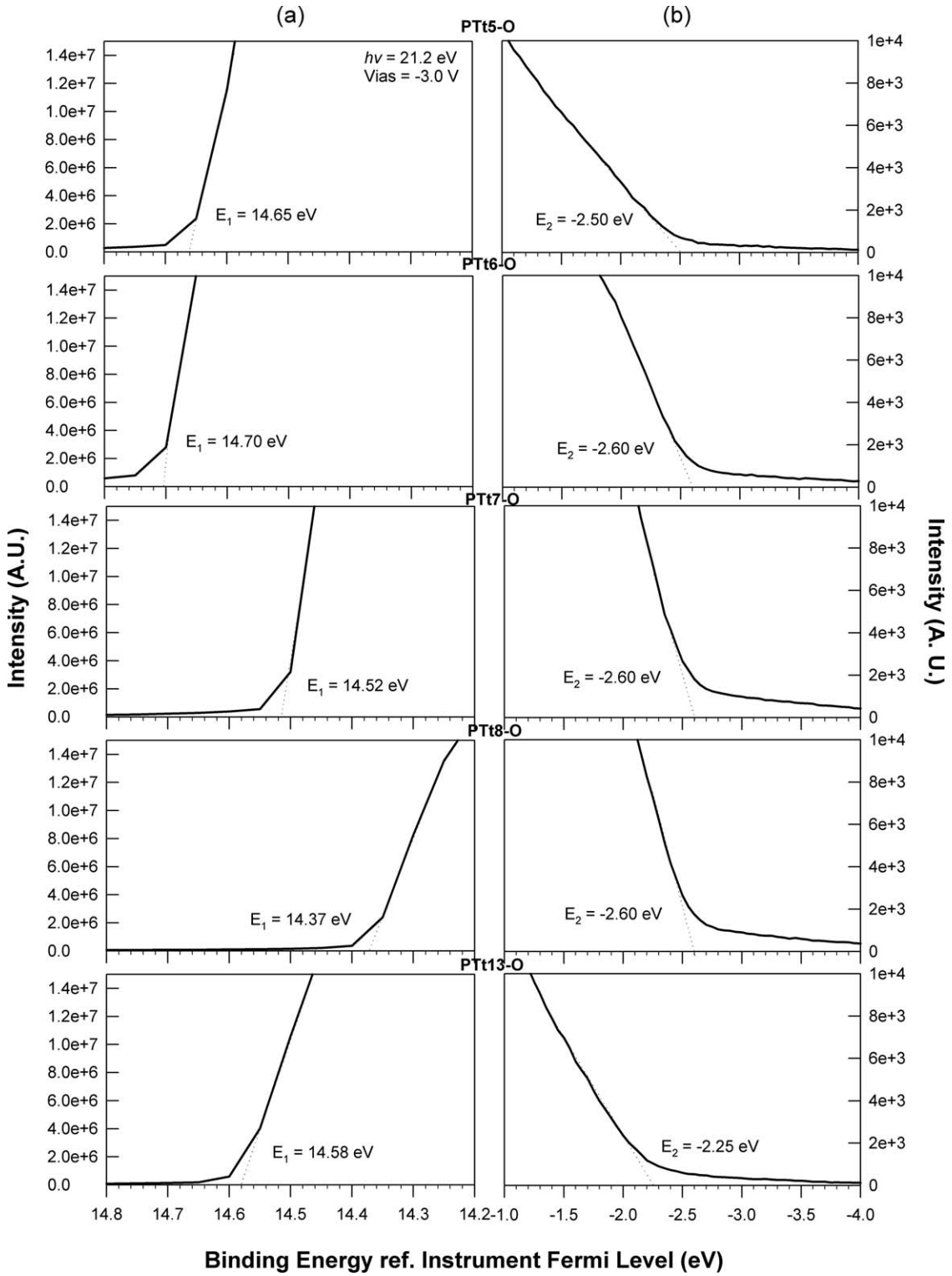

FIGURE 6 The UPS spectra of PTtx-O films on heavily doped silicon substrates. Panel (a) shows the low kinetic energy onset used to determine the secondary electron cutoff energy and the vacuum level; panel (b) shows the high kinetic energy onset used to determine the HOMO level energies. The incident photon energy was 21.2 eV, and the sample bias was −3 V.

temperatures (T_d) are summarized in Table 1. The first derivative of TGA curves shows no significant weight loss below 200 °C, which demonstrates that low-molecular-weight oligomers were completely eliminated by Soxhlet extraction. Two peaks ($Peak_{max}$ = ~350 and ~550 °C) in the first derivative curve of PTtx-O are due to the side-chain and

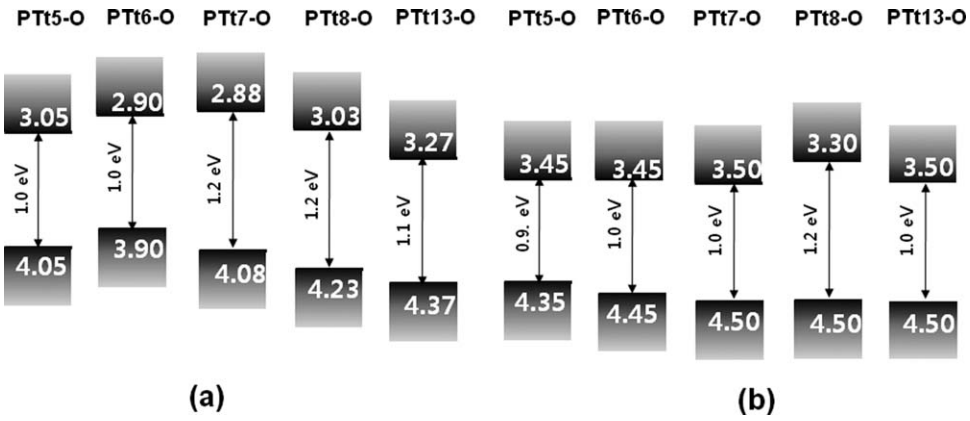

FIGURE 7 Schematic energy diagrams for PTtx-O (a) from UPS and UV–vis absorption measurements and (b) from electrochemical measurements.

main-chain degradation/decompositions, respectively (Supporting Information Figs. 7S and 8S). Interestingly, the first derivative curves of PTtx-G show only one peak ($Peak_{max}$ = ~450 °C), which implies that side-chain and main-chain degradations occur at the same temperature. The TGA analysis reveals that the onset points of 5% weight-loss temperature of PTtx are over 250 °C, which indicates that all of them have good thermal stability. We observed a very small onset weight loss starting at 150 °C in PTtx-O or in PTtx-G, but not as significant as reported in the literature.[24] Pomerantz et al. reported that the weight loss from 145 to 270 °C is attributed to side-chain cleavage, and they observed a 44% weight loss in case of poly(2-decylthieno[3,4-*b*]thiophene).[24] They also reported that poly(2-decylthieno[3,4-*b*]thiophene) is unstable at ambient condition, and the color turned from green-blue to dark gray upon standing, but PTtx synthesized in our hands by either $FeCl_3$ or GRIM polymerization has been very stable at ambient condition for several months, which has been verified by the UV–vis spectra and the GPC traces before and after aging being unchanged.

In conclusion, the low-bandgap monomers (Ttx) with various alkyl side chains were synthesized by a facile method in high yield compared to other reported methods for synthesis of thienothiophene derivatives. The PTtx polymers were synthesized by oxidative polymerization or GRIM polymerization. The results demonstrate that the alkyl (x = 5, 6, 7, 8, 13) substituents attached to the thienothiophene make the resulting polymer soluble in various organic solvents (THF, chloroform, and dichlorobenzene). Higher molecular weight PTtx with broader dispersity and lower molecular weight PTtx with narrower dispersity can be obtained by oxidative polymerization and GRIM polymerization, respectively. Side-chain length affects the optical properties of PTtx. As the side-chain length increases from five to seven, the wavelength of UV–vis–NIR absorption maximum decreases and bandgap increases, which can be explained by a steric hindrance effect of side chains, but with chain lengths over eight, solvation effect becomes much stronger and the wavelength of UV–vis–NIR absorption maximum decreases. The electronic structure of PTtx was also studied by UPS, and the band structure of PTtx was compared between electrochemistry measurement and optical measurement. The excellent thermal stability of the PTtx would render these low-bandgap polymers useful for applications in solar cells or thin-film transistors.

EXPERIMENTAL

Materials

3,4-Dibromothiophene, heptyne, octyne, nonyne, decyne, pentadecyne, diisopropylamine, *n*-BuLi in hexanes (2.6 M), and sulfur (S_8) were used as received from Alfa Aesar. Dichlorobis(triphenylphosphine)palladium(II) ($Pd(PPh_3)_2Cl_2$), copper(I) iodide, anhydrous methanol, anhydrous ether, anhydrous chlorobenzene, isopropyl-magnesium chloride·LiCl (*i*Pr-MgCl·LiCl), and $FeCl_3$ were used as received from Aldrich. *N*-Bromosuccinimide (NBS, Aldrich) was recrystallized from hot water. 1,3-Bis(diphenylphosphino)propane nickel(II) chloride ($Ni(dppp)Cl_2$) (Strem Chemicals) was also used as received. THF (Fisher Scientific) was used after distillation over sodium and benzophenone.

Synthesis of 3-Bromo-4-heptynyl (or octynyl, nonanyl, decynyl, pentadecynyl) Thiophene (BrThx) (1)

Dichlorobis (triphenylphosphine)palladium(II) ($Pd(PPh_3)_2Cl_2$) (1.45 g, 2.06 mmol) and CuI (0.396 g, 2.06 mmol) were added into a three-neck round-bottomed flask. After N_2 purging for 10 min, 3,4-dibromothiophene (10.0 g, 41.2 mmol), heptyne (or octyne, nonane, decyne, pentadecyne) (41.2 mmol), anhydrous methanol (40 mL), and diisopropylamine (40 mL) were added into the flask in sequence with N_2 purging. The solution was heated at 85 °C for 48 h. After solvent evaporation, the product mixture was poured into water and extracted with dichloromethane. The product was washed with $NaHCO_3$, water, and brine and dried over anhydrous $MgSO_4$ and filtered. After evaporation of the solvent under reduced pressure, the residue was further purified by column chromatography on silica gel with hexane, yielding a viscous light yellow liquid as a product.

BrTh5 (yield 72%): ^{1}H NMR (300 MHz, $CDCl_3$): δ (ppm) 7.34 (d, J = 3.5 Hz, 1H), 7.21 (d, J = 3.3 Hz, 1H), 2.44 (t, J = 6.7 Hz, 2H), 1.61 (m, 2H), 1.49 (m, 2H), 1.33 (m, 2H), 0.91 (t, J = 6.6 Hz, 3H). ^{13}C NMR (300 MHz, $CDCl_3$): δ (ppm) 14.06, 19.43, 22.25, 28.37, 31.06, 73.97, 93.67, 113.89,

122.57, 125.22, 127.78. Mass spectrum m/z 258.0 ($M^{\bullet+}$ + 1), 256.0 ($M^{\bullet+}$ − 1).

BrTh6 (yield 68%): ^{1}H NMR (300 MHz, $CDCl_3$): δ (ppm) 7.34 (d, J = 3.8 Hz, 1H), 7.21 (d, J = 3.1 Hz, 1H), 2.45 (t, J = 6.6 Hz, 2H), 1.61 (m, 2H), 1.49 (m, 2H), 1.35 (m, 4H), 0.90 (t, J = 6.9 Hz, 3H). ^{13}C NMR (300 MHz, $CDCl_3$): δ (ppm) 14.12, 19.46, 22.67, 28.55, 28.58, 31.37, 73.97, 93.67, 113.88, 122.56, 125.23, 127.76. Mass spectrum m/z 272.0 ($M^{\bullet+}$ + 1), 270.0 ($M^{\bullet+}$ − 1).

BrTh7 (yield 75%): ^{1}H NMR (300 MHz, $CDCl_3$): δ (ppm) 7.34 (d, J = 3.5 Hz, 1H), 7.21 (d, J = 3.1 Hz, 1H), 2.46 (t, J = 6.6 Hz, 2H), 1.62 (m, 2H), 1.50 (m, 2H), 1.37 (m, 6H), 0.91 (t, J = 6.7 Hz, 3H). ^{13}C NMR (300 MHz, $CDCl_3$): δ (ppm) 14.13, 19.45, 22.66, 28.55, 28.62, 28.83, 31.76, 73.92, 93.67, 113.88, 122.55, 127.75. Mass spectrum m/z 286.0 ($M^{\bullet+}$ + 1), 284.0 ($M^{\bullet+}$ − 1).

BrTh8 (yield 64%): ^{1}H NMR (300 MHz, $CDCl_3$): δ (ppm) 7.34 (d, J = 3.6 Hz. 1H), 7.21 (d, J = 3.3 Hz, 1H), 2.46 (t, J = 6.7 Hz, 2H), 1.61 (m, 2H), 1.44 (m, 2H), 1.32 (m, 8H), 0.87 (t, J = 6.9 Hz, 3H). ^{13}C NMR (300 MHz, $CDCl_3$): δ (ppm) 14.16, 19.46, 22.71, 28.62, 28.88, 29.14, 29.26, 31.88, 73.99, 93.67, 113.98, 122.55, 127.75. Mass spectrum m/z 300.0 ($M^{\bullet+}$ + 1), 298.0 ($M^{\bullet+}$ − 1).

BrTh13 (yield 60%): ^{1}H NMR (300 MHz, $CDCl_3$): δ (ppm) 7.34 (d, J = 3.8 Hz, 1H), 7.21 (d, J = 3.2 Hz, 1H), 2.46 (t, J = 6.4 Hz, 2H), 1.61 (m, 2H), 1.45 (m, 2H), 1.32 (m, 18H), 0.87 (t, J = 7.3 Hz, 3H). ^{13}C NMR (300 MHz, $CDCl_3$): δ (ppm) 14.16, 19.46, 22.72, 28.64, 28.88, 29.07, 29.10, 29.18, 29.22, 29.28, 29.45, 30.01, 32.03, 73.97, 93.67, 113.98, 122.55, 127.75. Mass spectrum m/z 369.0 ($M^{\bullet+}$ + 1), 367.0 ($M^{\bullet+}$ − 1).

Synthesis of 2-Pentyl (or Hexyl, Heptyl, Octyl, Tridecyl) Thieno[3,4-b]thiophene (Ttx) (2)

Under N_2 atmosphere, BrThx (**1**) (15.2 mmol) was dissolved in 35 mL of anhydrous diethyl ether. After cooling to −78 °C with acetone/dry ice bath, *n*-BuLi (8 mL of 2.6 M in hexane, 21.0 mmol) was added by syringe to the solution. After stirring for 1 h, the temperature was increased up to −35 °C with acetonitrile/dry ice bath. After further stirring for 1 h, sulfur powder (0.532 g, 16.5 mmol) was added to the solution and the temperature slowly raised to ambient with stirring for 3 h. After adding an excess amount of ethanol and filtration, the product was collected by rotary evaporation. The remaining viscous liquid was passed through a silica gel column with hexane.

Tt5 (yield 52%): ^{1}H NMR (300 MHz, $CDCl_3$): δ (ppm) 7.14 (s, 2H), 6.61 (s, 1H), 2.78 (t, *J* 7.5 Hz, 2H), 1.72 (m, 2H), 1.53 (m, 2H), 1.38 (m, 2H), 0.93 (t, J = 6.8 Hz, 3H). ^{13}C NMR (300 MHz, $CDCl_3$): δ (ppm) 13.98, 19.21, 22.46, 28.07, 30.03, 31.29, 110.04, 110.24, 113.22, 138.75, 147.58, 153.01. Mass spectrum m/z 210.1 ($M^{\bullet+}$).

Tt6 (yield 49%): ^{1}H NMR (300 MHz, $CDCl_3$): δ (ppm) 7.14 (s, 2H), 6.61 (s, 1H), 2.78 (t, J = 7.2 Hz, 2H), 1.73 (m, 2H), 1.39 (m, 6H), 0.94 (t, J = 6.6 Hz, 3H). ^{13}C NMR (300 MHz, $CDCl_3$): δ (ppm) 14.14, 19.25, 22.62, 28.57, 30.32, 31.62, 110.03, 110.24, 113.21, 138.76, 147.58, 153.82. Mass spectrum m/z 224.1 ($M^{\bullet+}$).

Tt7 (yield 46%): ^{1}H NMR (300 MHz, $CDCl_3$): δ (ppm) 7.14 (s, 2H), 6.61 (s, 1H), 2.78 (t, J = 7.0 Hz, 2H), 1.72 (m, 2H), 1.32 (m, 8H), 0.95 (t, J = 6.7 Hz, 3H). ^{13}C NMR (300 MHz, $CDCl_3$): δ (ppm) 14.18, 19.26, 22.72, 28.48, 29.16, 30.37, 31.95, 110.04, 110.24, 113.22, 130.77, 147.59, 153.03. Mass spectrum m/z 238.1 ($M^{\bullet+}$).

Tt8 (yield 43%): ^{1}H NMR (300 MHz, $CDCl_3$): δ (ppm) 7.14 (s, J = 7.3 Hz, 2H), 6.61 (s, 1H), 2.73 (t, 2H), 1.68 (m, 2H), 1.38 (m, 10H), 0.96 (t, J = 6.9 Hz, 3H). ^{13}C NMR (300 MHz, $CDCl_3$): δ (ppm) 14.22, 21.27, 22.77, 28.92, 30.44, 31.41, 32.01, 38.96, 110.10, 110.30, 113.28, 138.84, 147.66, 153.09. Mass spectrum m/z 252.1 ($M^{\bullet+}$).

Tt13 (yield 54%): ^{1}H NMR (300 MHz, $CDCl_3$): δ (ppm) 7.14 (s, 2H), 6.61 (s, 1H), 2.73 (t, J = 7.5 Hz, 2H), 1.68 (m, 2H), 1.38 (m, 20H), 0.96 (t, J = 7.2 Hz, 3H). ^{13}C NMR (300 MHz, $CDCl_3$): δ (ppm) 14.17, 20.73, 22.78, 25.31, 29.14, 29.41, 29.58, 29.69, 30.35, 31.63, 31.94, 31.96, 34.56, 110.01, 110.21, 113.19, 138.77, 147.59, 153.02. Mass spectrum m/z 322.2 ($M^{\bullet+}$).

Dibromination of Ttx (Br-Ttx-Br)

Ttx (1 mmol) was dissolved in 15 mL THF, to which NBS (0.36g, 2 mmol) was added in the dark. After stirring the mixture at room temperature for 3 h, the solvent was removed under reduced pressure. The residue was purified by column chromatography on silica gel (hexane as an eluent) to yield the yellowish viscous product.

Br-Tt5-Br (yield 82%): ^{1}H NMR (300 MHz, $CDCl_3$): δ (ppm) 6.48 (s, 1H), 2.72 (t, J = 7.4, 2H), 1.66 (m, 2H), 1.37 (m, 4H), 0.93 (t, J = 6.5 Hz, 3H).

Br-Tt6-Br (yield 83%): ^{1}H NMR (300 MHz, $CDCl_3$): 6.48 (s, 1H), 2.72 (t, J = 7.4 Hz, 2H), 1.68 (m, 2H), 1.35 (m, 6H), 0.94 (t, J = 6.6 Hz, 3H).

Br-Tt7-Br (yield 78%): ^{1}H NMR (300 MHz, $CDCl_3$): 6.48 (s, 1H), 2.72 (t, J = 7.5 Hz, 2H), 1.68 (m, 2H), 1.33 (m, 8H), 0.94 (t, J = 6.8 Hz, 3H).

Br-Tt8-Br (yield 88%): ^{1}H NMR (300 MHz, $CDCl_3$): 6.49 (s, 1H), 2.73 (t, J = 7.4 Hz, 2H), 1.70 (m, 2H), 1.31 (m, 10H), 0.93 (t, J = 6.8 Hz, 3H).

Br-Tt13-Br (yield 85%): ^{1}H NMR (300 MHz, $CDCl_3$): 6.49 (s, 1H), 2.72 (t, J = 7.5 Hz, 2H), 1.69 (m, 2H), 1.31 (m, 20H), 0.93 (t, J = 7.0 Hz, 3H).

Oxidative Polymerization of PTtx (3)

To a suspension of $FeCl_3$ (0.162 g, 1.0 mmol) in 10 mL of chlorobenzene, Ttx (1.0 mmol) in 10 mL of chlorobenzene was added dropwise over 30 min under nitrogen atmosphere. After stirring the mixture at room temperature for 1 h, the solvent was removed under reduced pressure. The polymer was precipitated by addition of excess amount of methanol/water (80/20 v/v) and then washed with water and methanol several times. The powder was dispersed in

chloroform/methanol/NH_4OH aq. soln. (30%) and then stirred for 5 h. After filtration, the crude product was then subjected to Soxhlet extraction with methanol, acetone, hexane, and chloroform. The chloroform solution was added by some portion of hydrazine hydrate and stirred overnight. The polymer was precipitated by addition of excess amount of methanol/water (80/20 v/v) and then washed with water and methanol several times to afford a dark bluish solid. The polymer was dried under vacuum at 60 °C for 12 h.

PTt5 (yield 53%): ^{1}H NMR (300 MHz, $CDCl_3$): δ (ppm) 7.8–6.6 (m, 1H), 3.1–2.5 (m, 2H), 1.9–1.6 (m, 2H), 1.6–1.0 (m, 4H), 1.0–0.5 (m, 3H).

PTt6 (yield 66%): ^{1}H NMR (300 MHz, $CDCl_3$): 7.8–6.6 (m, 1H), 3.1–2.6 (m, 2H), 1.9–1.6 (m, 2H), 1.6–1.1 (m, 6H), 1.1–0.5 (m, 3H).

PTt7 (yield 49%): ^{1}H NMR (300 MHz, $CDCl_3$): 7.7–6.8 (m, 1H), 3.1–2.5 (m, 2H), 2.0–1.6 (m, 2H), 1.6–1.1 (m, 8H), 1.1–0.4 (m, 3H).

PTt8 (yield 33%): ^{1}H NMR (300 MHz, $CDCl_3$): 7.7–6.8 (m, 1H), 3.1–2.5 (m, 2H), 1.9–1.6 (m, 2H), 1.6–1.1 (m, 10H), 1.1–0.6 (m, 3H).

PTt13 (yield 41%): ^{1}H NMR (300 MHz, $CDCl_3$): 7.7–6.8 (m, 1H), 3.1–2.5 (m, 2H), 1.9–1.6 (m, 2H), 1.6–1.1 (m, 20H), 1.1–0.6 (m, 3H).

GRIM Polymerization of PTtx

A solution of Br-Ttx-Br (1 mmol) and *i*Pr-MgBr·LiCl (0.77 mL of 1.0 M in THF, 1 mmol) was added to 25 mL of anhydrous THF under nitrogen. The reaction mixture was stirred at room temperature for 2 h. Ni(dppp)Cl_2 (6 mg, 0.01 mmol) was added to the reaction mixture under nitrogen. The polymerization was allowed to proceed for 48 h at room temperature followed by quenching of the reaction mixture with MeOH/water. The precipitated polymer was filtered through a thimble and subjected to Soxhlet extraction with methanol, acetone, hexane, and chloroform. After solvent evaporation, the polymer was dried under vacuum for 12 h. To the chloroform solution was added a small portion of hydrazine hydrate and stirred overnight. The polymer was precipitated by addition of excess amount of methanol/water (80/20 v/v) and then washed with water and methanol several times to afford a dark bluish solid. The polymer was dried under vacuum at 60 °C for 12 h. Yield: 23, 16, 20, and 17% (PTt5, PTt6, PTt7, and PTt8, respectively). The ^{1}H NMR spectra of PTtx synthesized by GRIM polymerization are identical with those of PTtx synthesized by oxidative polymerization.

Measurement

The chemical structures of materials used in this study were identified by ^{1}H NMR and ^{13}C NMR (Advance DPX-300). Molecular weight and dispersity were measured by gel permeation chromatography equipped with a refractive index detector using $CHCl_3$ or THF as an eluent, and the columns were calibrated against standard PS. The optical absorption spectra were obtained by UV–vis–NIR spectrophotometer (Lambda 850, Perkin-Elmer). DLS was performed on a Malvern Zetasizer Nano-ZS. Cyclic voltammetry experiments were carried out on potentiostat/galvanostat (Model 273A, EG&G Princeton Applied Research) in an electrolyte solution of 0.1 M Bu_4NPF_6 in dichloromethane. A three-electrode cell was used for all experiments. Platinum wires (Bioanalytical System) were used as both counter and working electrodes, and silver/silver ion (Ag in 0.1 M $AgNO_3$ solution, Bioanalytical System) was used as a reference electrode. TGA was carried out using a Mettler Toledo TGA/SDTA851e thermogravimetric analyzer with a heating rate of 10 °C/min from room temperature to 700 °C under N_2 purge.

The UPS measurements were performed with the Electron Spectroscopy for Chemical Analysis instrument (Omicron Nanotechnology, model ESCA+S) at a base pressure of 4×10^{-10} mbar. The instrument configuration consisted of a helium discharge lamp (He I line, 21.2 eV) as the UV excitation source and a hemispherical SPHERA energy analyzer. The energies of the HOMO levels of the studied polymer films were determined from the UPS measurements. The procedure consisted of two steps. First, the secondary electron cutoff energy was determined as the intersection of a tangent line to the low kinetic energy onset of the UPS spectrum with the abscissa axis. The vacuum level of a polymer film was taken to be 21.2 eV away from the secondary electron cutoff energy. Second, the HOMO level was determined from the intersection of a tangent line to the high kinetic energy onset of the UPS spectrum with the abscissa axis. The previously determined vacuum level was taken as the absolute reference point of the energy scale. All the measurements were done at a −3 V sample bias to collect the low kinetic energy electrons. The resolution of the UPS instrument was 0.1 eV as determined from the width of the Fermi level of silver.

Thin polymer films for UPS measurements were spin coated onto a silver-coated (80-nm-thick) highly doped (resistivity of 0.001–0.005 Ω cm) silicon substrate or directly onto a highly doped silicon substrates in a glove box (nitrogen as a base gas, <2 ppm of moisture, <10 ppm of O_2) and exposed to ambient air for less than 30 s during their transfer from the glove box to the UPS instrument. Subsequently, the films were immediately degassed in high vacuum and ultra-high vacuum for at least an hour before the measurements. The thicknesses of polymer films were kept below 10 nm as determined by the surface profiler (KLA Tencor, model Alpha-Step IQ).

CONCLUSIONS

In conclusion, the low-bandgap monomers (Ttx) with various alkyl side chains were synthesized by a facile method in high yield compared to other reported methods for synthesis of thienothiophene derivatives. The PTtx polymers were synthesized by oxidative polymerization or GRIM polymerization. The results demonstrate that the alkyl (x = 5, 6, 7, 8, 13) substituents attached to the thienothiophene make the resulting polymer soluble in various organic solvents (THF, chloroform, and dichlorobenzene). Higher molecular weight PTtx with broader dispersity and lower molecular weight

PTtx with narrower dispersity can be obtained by oxidative polymerization and GRIM polymerization, respectively. Side-chain length affects the optical properties of PTtx. As the side-chain length increases from five to seven, the wavelength of UV–vis–NIR absorption maximum decreases and bandgap increases, which can be explained by a steric hindrance effect of side chains, but with chain lengths over eight, solvation effect becomes much stronger and the wavelength of UV–vis–NIR absorption maximum decreases. The electronic structure of PTtx was also studied by UPS, and the band structure of PTtx was compared between electrochemistry measurement and optical measurement. The excellent thermal stability of the PTtx would render these low-bandgap polymers useful for applications in solar cells or thin-film transistors.

Funding from the Center for UMass-Industry Research on Polymers Energy Cluster is gratefully acknowledged. W.J. Bae and W.H. Jo thank the Korea Research Foundation for financial support through the Global Research Laboratory (GRL) program. This material is based upon work supported as part of Polymer-Based Materials for Harvesting Solar Energy, an Energy Frontier Research Center funded by the U.S. Department of Energy, Office of Science, Office of Basic Energy Sciences under Award Number DE-SC0001087. Mass spectral data were obtained at the University of Massachusetts Mass Spectrometry Facility, which is supported, in part, by National Science Foundation.

REFERENCES AND NOTES

1 Burroughes, J. H.; Bradley, D. D. C.; Brown, A. R.; Marks, R. N.; Mackay, K.; Friend, R. H.; Burn, P. L.; Holmes, A. B. Nature 1990, 347, 539–541.

2 Tessler, N.; Denton, G. J.; Friend, R. H. Nature 1996, 382, 695–697.

3 Zaumseil, Y.; Sirringhaus, H. Chem Rev 2007, 107, 1296–1323.

4 Halls, J. J. M.; Walsh, C. A.; Greenham, N. C.; Marseglia, E. A.; Friend, R. H.; Moratti, S. C.; Holmes, A. B. Nature 1995, 376, 498–500.

5 Yu, G.; Gao, J.; Hummelen, J. C.; Wudl, F.; Heeger, A. J. Science 1995, 270, 1789–1791.

6 Roncali, J. Chem Rev 1997, 97, 173–206.

7 Sotzing, G. A.; Lee, K. Macromolecules 2002, 35, 7281–7286.

8 Thompson, B. C.; Fréchet, J. M. J. Angew Chem Int Ed 2008, 47, 58–77.

9 Hergué, N.; Mallet, C.; Frére, P.; Allain, M.; Roncali, J. Macromolecules 2009, 42, 5593–5599.

10 Scharber, M. C.; Muehlbacher, D.; Koppe, M.; Denk, P.; Waldauf, C.; Heeger, A. J.; Brabec, C. J. Adv Mater 2006, 18, 789–794.

11 Zhang, F.; Mammo, W.; Andersson, L. M.; Admassie, S.; Andersson, M. R.; Inganäs, O. Adv Mater 2006, 18, 2169–2173.

12 Cheng, Y.-J.; Yang, S.-H.; Hsu, C.-S. Chem Rev 2009, 109, 5868–5923.

13 Ajayaghosh, A. Chem Soc Rev 2003, 32, 181–191.

14 Skotheim, T. A.; Reynolds, J. R. Handbook of Conducting Polymers, 3rd ed.: Conjugated Polymers, Theory, Synthesis, Properties, and Characterization; CRC Press LLC: Boca Raton, FL, 2007.

15 Zhang, S.; Guo, Y.; Fan, H.; Liu, Y.; Chen, H.-Y.; Yang, G.; Zhan, X.; Liu, Y.; Li, Y.; Yang, Y. J Polym Sci Part A: Polym Chem 2009, 47, 5498–5508.

16 Zhang, S.; Fan, H.; Liu, Y.; Zhaon, G.; Li, Q.; Li, Y.; Zhan, X. J Polym Sci Part A: Polym Chem 2009, 47, 2843–2852.

17 Lee, T. W.; Kang, N. S.; Yu, J. W.; Hoang, M. H.; Kim, K. H.; Jin, J.-I.; Choi, D. H. J Polym Sci Part A: Polym Chem 2010, 48, 5921–5929.

18 Kmínek, I.; Výprachtický, D.; Kříž, J.; Dybal, J.; Cimrová, V. J Polym Sci Part A: Polym Chem 2010, 48, 2743–2756.

19 Amir, E.; Sivanandan, K.; Cochran, J. E.; Cowart, J. J.; Ku, S.-Y.; Seo, J. H.; Chabinyc, M. L.; Hawker, C. J. J Polym Sci Part A: Polym Chem 2011, 49, 1933–1941.

20 Lee, K.; Sotzing, G. A. Macromolecules 2001, 34, 5746–5747.

21 Lian, Y.; Wu, Y.; Feng, D.; Tsai, S.-T.; Son, H.-J.; Li, G.; Yu, L. J Am Chem Soc 2009, 131, 56–57.

22 Hou, J.; Chem, H.-Y.; Zhan, S.; Chen, R. I.; Yang, Y.; Wu, Y.; Li, G. J Am Chem Soc 2009, 131, 15586–15587.

23 Pomerantz, M.; Gu, X. Synth Met 1997, 84, 243–244.

24 Pomerantz, M.; Gu, X.; Zhang, S. X. Macromolecules 2001, 34, 1817–1822.

25 Lee, B.; Sehadri, V.; Palko, H.; Sotzing, G. A. Adv Mater 2005, 17, 1792–1795.

26 Brandsma, L.; Verkruijsse, H. D. Synth Commun 1990, 20, 2275–2277.

27 Lee, W. S.; Park, J. H.; Baek, M.-J.; Lee, Y.-S.; Lee, S.-H.; Pyo, M.; Zong, K. Synth Met 2010, 160, 1368–1371.

28 Park, J. H.; Seo, Y. G.; Yoon, D. H.; Lee, Y.-S.; Lee, S.-H.; Pyo, M.; Zong, K. Eur Polym J 2010, 46, 1790–1795.

29 Sheina, E. E.; Liu, J.; Iovu, M. C.; Laird, D. W.; McCullough, R. D. Macromolecules 2004, 37, 3526–3528.

30 Iovu, M. C.; Sheina, E. E.; Gil, R. R.; McCullough, R. D. Macromolecules 2005, 38, 8649–8656.

31 Stefan, M. C.; Javier, A. E.; Osaka, I.; McCullough, R. D. Macromolecules 2009, 42, 30–32.

32 McCullough, R. D.; Lowe, R. D.; Jayaraman, M.; Anderson, D. L. J Org Chem 1993, 58, 904–912.

33 McCullough, R. D.; Tristram-Nagle, S.; Williams, S. P. J Am Chem Soc 1993, 115, 4910–4911.

34 Trad, H.; Ltaief, A.; Majdoub, M.; Bouazizi, A.; Davenas, J. Mater Sci Eng C 2006, 26, 340–343.

35 Li, Y. F.; Cao, Y.; Gao, J.; Wang, D. L.; Yu, G.; Heeger, A. J. Synth Met 1999, 99, 243–248.

36 Schulz, B.; Janietz, S. Curr Trends Polym Sci 1996, 1, 1–5.

37 Osaheni, J.; Jenekhe, S. A. J Am Chem Soc 1995, 117, 7389–7398.

38 Kanai, K.; Miyazaki, T.; Suzuki, H.; Inaba, M.; Ouch, Y.; Seki, K. Phys Chem Chem Phys 2010, 12, 273–282.

39 Kanai, K.; Miyazaki, T.; Suzuki, H.; Inaba, M. Phys Chem Chem Phys 2010, 12, 273–282.

40 Rieβ, E. G. Adv Technol 1997, 8, 381–391.

41 Brien, D. O.; Bleyer, A.; Lidzey, D. G.; Bradley, D. D. C.; Tsutsui, T. J Appl Phys 1997, 82, 2662–2670.

42 Janietz, S.; Bradley, D. D. C.; Grell, M.; Giebeler, C.; Inbasekaran, M.; Woo, E. P. Appl Phys Lett 1998, 73, 2453–2455.

43 D'Andrade, B. W.; Datta, S.; Forrest, S. R.; Djurovich, P.; Polikarpov, E.; Thompson, M. E. Org Electron 2005, 6, 11–20.

44 Djurovich, P. I.; Mayo, E. I.; Forrest, S. R.; Thompson, M. E. Org. Electron 2009, 10, 515–520.

45 Gu, X. Ph.D. Dissertation, The University of Texas at Arlington, Arlington, TX, 1995.

46 Neef, C. J.; Brotherston, I. D.; Ferraris, J. P. Chem Mater 1999, 11, 1957–1958.

47 The ionization potential of Si was taken as a sum of electron affinity and bandgap energy at room temperature, 4.05 eV (Sze, S. M. Physics of Semiconductor Devices; Wiley, 1969) and 1.12 eV (Herman, F. Proc Inst Radio Eng 1955, 43, 1703), respectively.

48 Chelvayohan, M.; Mee, C. H. B. J Phys C: Solid State Phys 1982, 15, 2305–2312.